Effect of doping and oxygen vacancies on the octahedral tilt transitions in the $BaCeO_3$ perovskite

F. Cordero,[1] F. Trequattrini,[2] F. Deganello,[3] V. La Parola,[3] E. Roncari,[4] and A. Sanson[4]
[1]*CNR-Istituto dei Sistemi Complessi (ISC), Area della Ricerca di Roma-Tor Vergata, Via del Fosso del Cavaliere 100, I-00133 Roma, Italy*
[2]*Dip. Fisica, Università di Roma "La Sapienza", P.le A. Moro 5, I-00184 Roma, Italy*
[3]*CNR-Istituto per lo Studio dei Materiali Nanostrutturati (ISMN), Via Ugo La Malfa 153, I-90146 Palermo, Italy*
[4]*CNR-Istituto di Scienza e Tecnologia dei Materiali Ceramici (ISTEC), Via Granarolo 64, I-48018 Faenza, Italy*
(Received 23 July 2010; published 1 September 2010)

We present a systematic study of the effect of Y doping and hydration level on the structural transformations of $BaCeO_3$ based on anelastic spectroscopy experiments. The temperature of the intermediate transformation between rhombohedral and orthorhombic *Imma* phases rises with increasing the molar fraction x of Y roughly as $(500\ \mathrm{K})\times x$ in the hydrated state, and is depressed of more than twice that amount after complete dehydration. This is explained in terms of the effect of doping on the average (Ce/Y)-O and Ba-O bond lengths, and of lattice relaxation from O vacancies. The different behavior of the transition to the lower temperature *Pnma* orthorhombic phase is tentatively explained in terms of progressive flattening of the effective shape of the OH^- ion and ordering of the O vacancies during cooling.

DOI: 10.1103/PhysRevB.82.104102 PACS number(s): 61.72.J−, 63.70.+h, 62.40.+i, 66.10.Ed

I. INTRODUCTION

The $BaCeO_3$ perovskite undergoes three phase transformations starting from the high-temperature cubic (C) phase: to rhombohedral (R) at $T_1=1170$ K, to orthorhombic *Imma* (O1) at $T_2=670$ K, and to orthorhombic *Pnma* (O2) at $T_3=563$ K, as determined by neutron diffraction[1] and by combined differential scanning calorimetry, dilatometry, and x-ray diffraction (XRD).[2] The sequence of phase transformations and the various structures are well characterized in the undoped state of $BaCeO_3$, and even a quantitative description of the spontaneous strains by means of the Landau expansion of the free energy has been presented.[3] Instead, the situation is confused when a trivalent dopant, e.g., Y^{3+}, is substituted into the Ce^{4+} place in order to make the material a protonic conductor. The understanding of the influence of doping on the phase transitions in the perovskite ionic conductors is not only of academic interest. In fact, the occurrence of phase transformations, especially if accompanied by ordering of the mobile ionic species, protons, and O vacancies, is closely related to the mobility of such ions and to the durability of the material in applications like fuel cells or membranes for gas separation.[4–7] Although various indications have been reported that the transition temperatures in $BaCeO_3$ depend on doping and on the hydration state,[1,8–13] no systematic study and analysis has appeared yet. According to Raman spectroscopy measurements on variously doped $BaCeO_3$, the room-temperature structure changes to the more symmetric tetragonal and cubic phases with increasing Nd^{3+} substitution[10] but a subsequent neutron-diffraction experiment excludes any significant influence on the room-temperature orthorhombic structure from Nd doping.[11] For $BaCe_{1-x}Y_xO_{3-\delta}$ (BCY), a change from the O2 to the R structure at room temperature was found at $x\geq 0.2$ with neutron diffraction,[12] whereas a later x-ray diffraction study did not show such a transition to rhombohedral at room temperature but rather impurity phases arising from a more limited Y solubility range.[13,14] More recently, anelastic spectroscopy measurements on BCY showed that passing from the hydrated to the outgassed state with $x=0.1$ lowers the temperature of the O1-R transition by as much as 250 K.[15] Here we present a more extensive study of the effect of doping and O vacancies (V_O) on the phase transitions in BCY, again based on anelastic measurements. An interpretation of the observations is proposed, assuming that the driving force for the octahedral tilting instabilities is the mismatch between too long *A*-O and too short *B*-O bonds, as usual for ABO_3 perovskites; a minimal model is adopted for the changes with doping and hydration level of the tolerance factor and of the lattice relaxation due to V_O.

II. EXPERIMENTAL

The samples of $BaCe_{1-x}Y_xO_3$ with $x=0$, 0.02, 0.1, 0.15, and 0.3 were prepared as already described,[16] with starting powders obtained by autocombustion synthesis,[17] followed by crystallization in air at 1273 K for 5 h. No oxide impurity phases were detected by XRD after synthesis for $x\leq 0.15$. The sample with nominal $x=0.3$ was not monophasic since the solubility limit of Y in BCY is lower than 0.3. In fact, impurity phases are detected by XRD for $x\geq 0.2$ (Ref. 13) and by EXAFS for $x\geq 0.17$.[14] We did not determine the exact concentration of Y in solid solution in the $x=0.3$ sample and in what follows we will set this value to $x=0.2$. The powders were first uniaxially pressed at 50 MPa and then isostatically pressed at 200 MPa obtaining $60\times 7\times 6$ mm^3 ingots, which were sintered at 1773 K for 10 h. The samples were cut as thin bars about 1 mm thick and ~4 cm long. In order to make them conducting for the anelastic experiments, their faces were covered with Ag paint or Pt paint when temperatures higher than 900 K had to be reached. We tried with SPI-Chem Conductive Platinum Paint consolidated at 1270 K, or with 1000 Å of Pt magnetron sputtered directly on the sample surface. Unfortunately, none of these electrodes resisted the anelastic measurements in vacuum $<10^{-5}$ mbar in the temperature range 1000–1300 K since in

all cases they evaporated away. This fact rendered the measurements at >1000 K difficult, and we could not obtain extensive and reliable data on the R-C transition near 1200 K.

Hydration was achieved by maintaining the samples for 1–2 h at 793 K in a static atmosphere of 50–100 mbar H_2O, followed by slow cooling, while outgassing was achieved in vacuum $<10^{-5}$ mbar up to 1000 K or during the anelastic experiments. The resulting variations in the gaseous contents were monitored from the change in weight. The reaction of equilibrium of the O deficient perovskite with water vapor is $H_2O+V_O^{\bullet\bullet}+O_O^{\times}\leftrightarrow 2OH_O^{\bullet}$,[4] where a molecule of water fills one V_O and provides two protons that may diffuse among O^{2-}, to which are bound as peroxide ions $(OH)^-$. The superscript dots represent excess $+e$ charges of the species with respect to the perfect lattice in Kröger-Vink notation. According to this reaction, the concentration of V_O in $BaCe_{1-x}Y_xO_{3-\delta}H_y$ can vary within $\delta \leq x/2$ and concomitantly the concentration y of protons within $y \leq x$. It was found that the maximum possible hydration was ~15% lower than the theoretical maximum of $y=x$; this is usual in the doped cerate and zirconate perovskites, and can be due to partial occupation of the Ba sites by the trivalent dopants or to other defects.

The Young's modulus E was measured by electrostatically exciting the flexural modes of the bars suspended in vacuum on thin thermocouple wires in correspondence with the nodal lines. Besides the first flexural mode, the third and sometimes the fifth modes, with frequencies 5.4 and 13.3 times higher, could be measured during the same run; the frequency of the fundamental mode was $\omega/2\pi \simeq 1.5-3$ kHz, depending on the sample shape and state. The data will be presented as real part s' of the elastic compliance $s(\omega,T)=s'-is''=E^{-1}$, referred to its extrapolation s_0 to 0 K, and elastic energy-loss coefficient $Q^{-1}=s''/s'$. The first is proportional to the square of the sample resonance frequency, $s'(T) \propto \omega^2(T)$, and presents peaks or steps at the structural phase transformations; the latter was measured from the decay of the free oscillations or from the width of the resonance peak, and presents peaks due to the relaxational motion of point and extended defects[18] (V_O, protons and their complexes with dopants, twin walls, etc.). For an elementary relaxation process it is[18]

$$\delta s(\omega,T) = \frac{\Delta}{T}\frac{1}{1+i\omega\tau} \tag{1}$$

with maximum at the temperatures at which the defect relaxation time $\tau \sim \omega^{-1}$. Since $\tau(T)$ is a decreasing function of temperature, usually according to the Arrhenius law, the temperature of a thermally activated peak increases with frequency. The peaks due to the hopping of V_O and to the reorientation of protons around Y dopants have already been identified,[15,16] and allow one to monitor the concentrations of such defects and to study their dynamics.

III. RESULTS

Figure 1 presents the anelastic spectrum of a sample of undoped $BaCeO_3$ measured at two frequencies: 1.6 and 8.4 kHz. The real parts s' are practically coincident at both

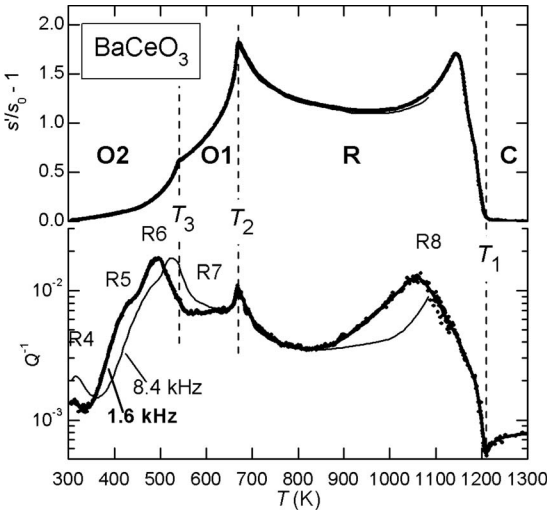

FIG. 1. Real part of the elastic compliance (upper panel) and elastic energy-loss coefficient (lower panel) of undoped $BaCeO_3$, measured at 1.6 and 8.4 kHz.

frequencies and present sharp steps or peaks in correspondence with the three phase transformations at $T_1=1210$ K, $T_2=668$ K, and $T_3=540$ K. These temperatures are close to those determined by neutron diffraction[1] and define the temperature ranges of the cubic, rhombohedral, and two orthorhombic phases. We identify T_1 of the R-C transformation with the temperature of the kink between almost flat and sharply rising compliance, rather than with the peak at a temperature 65 K lower. This also coincides with a sharp dip in the absorption. Such a dip is rather anomalous, since usually one finds a peak or more or less rounded step at the onset of a structural transformation, but it clearly separates the rhombohedral region, with absorption due to the motion of domain walls, from the cubic region without appreciable anelastic losses.

The elastic energy-loss coefficient, besides clear anomalies in correspondence with the transitions, has five relaxation peaks in the 300–1300 K temperature range, labeled R4–R8 because there are other relaxation processes at lower temperatures (see Ref. 16 and Fig. 4 later on). The thermally activated character of these processes is clear from the fact that they are shifted to higher temperature at the higher frequency [see Eq. (1)].

Figure 2 presents a series of anelastic spectra of a sample of $BaCe_{1-x}Y_xO_3$ with $x=0.10$ at various stages of hydration, from fully hydrated (thick black lines) to fully outgassed (light gray); these spectra have already been published in a preliminary study[15] of the effect of varying hydration on the structural and elastic properties of BCY. The two $Q^{-1}(T)$ peaks at lower temperature are labeled as RH and RV since they are due to hopping of protons, likely around Y dopants,[16] and of V_O, respectively. Their evolution allows us to confirm that the sample passes from fully hydrated (RV is absent and RH saturated) to fully outgassed (RH is absent and RV saturated). The presence of the intermediate curves (only few of them are reported) allows us to ascertain that indeed outgassing shifts the transition at T_2 of 250 K to lower temperature, while the transition at T_3 is soon smeared

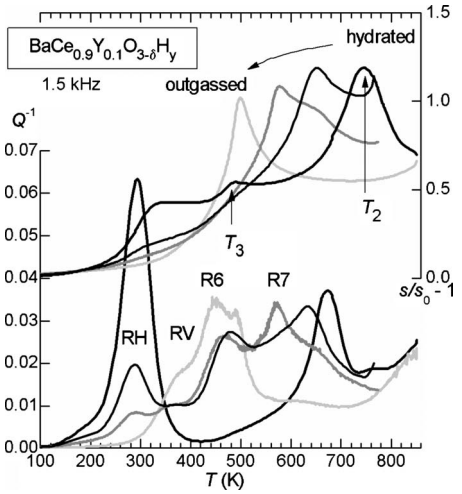

FIG. 2. Real part of the elastic compliance (upper panel) and elastic energy-loss coefficient (lower panel) of $BaCe_{1-x}Y_xO_{3-\delta}H_y$ with $x=0.1$, measured at ~1.5 kHz at various hydration levels, from fully hydrated (black) to fully outgassed (light gray).

and masked by the presence of the former transition, but does not seem to shift appreciably.

The effect of Y^{3+} doping on the phase transformations at T_2 and T_3 is shown in Fig. 3, where the elastic compliance curves are plotted of samples having $x=0$, 0.02, 0.10, 0.15, and 0.2 in the fully hydrated and fully outgassed states. There is no outgassed curve at $x=0.2$ because the sample broke after the first measurement. With increasing doping, and hence lattice disorder, there is progressive smearing of the peaks at the transitions, so that T_3 becomes more and more difficult to determine. This is especially true in the outgassed state, where the transition at T_2, whose effects on the elastic compliance are prevalent, shifts consistently to

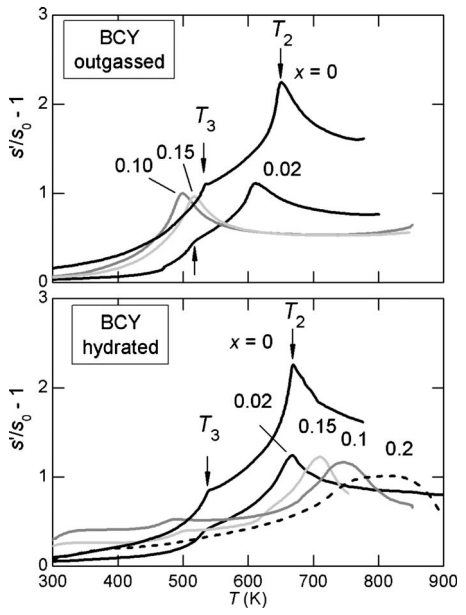

FIG. 3. Real part of the elastic compliance of a series of samples with different doping x measured in the hydrated and outgassed states.

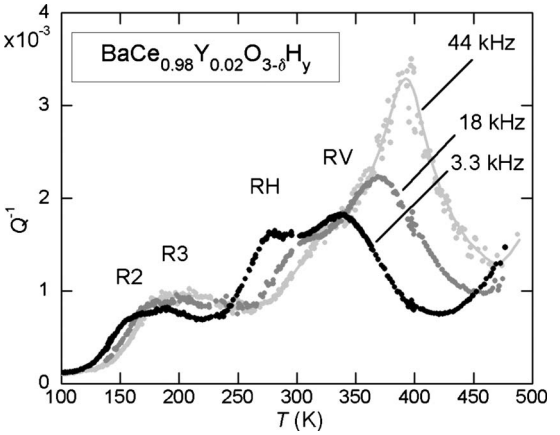

FIG. 4. Elastic energy-loss coefficient of BCY with $x=0.02$ in an intermediate hydration state, measured at three frequencies.

lower temperature and masks the effects of the O2-O1 transition. Note that there is an inversion in the trend of the anelastic spectra between $x=0.1$ and 0.15, as discussed later. The transition temperatures deduced from these curves will be plotted in Fig. 5.

We finally present an example of $Q^{-1}(T)$ curves measured at three different frequencies, where it is particularly clear that the dynamics of the V_O is not simply that of independent defects, which would give rise to a Debye relaxation, Eq. (1), but seems to have an important contribution from cooperative effects, possibly connected with V_O ordering in the O2 phase. The $Q^{-1}(\omega,T)$ curves in Fig. 4 are measured at 3.3, 18, and 44 kHz on a sample with $x=0.02$ in an intermediate state of hydration where both V_O and H are present. Among the various peaks, with the help of Fig. 2 we recognize RH, probably due to reorientation of H about Y dopants[16] while RV is certainly due to V_O, although it is not yet determined whether trapping by Y has a role. The interesting feature in Fig. 4 is that the intensity of peak RV is a drastically increasing function of temperature, instead of having the $1/T$ dependence expected from Eq. (1). The effect is not due to O loss during the measurements in vacuum, since the curves at different frequencies are measured during a same run, and we have abundant data showing that the $Q^{-1}(T)$ are perfectly reproducible until one does not exceed 500 K. We mention that also the relaxation peak R6 in Fig. 2 displays a similar behavior, although the divergence of its intensity on approaching T_3 might be partially due to overlapping with the narrow dissipation peak associated with the structural transition. We did not make a thorough analysis of these complicated anelastic spectra and cannot say yet whether R6 involves V_O, twin walls, or both; it certainly appears that the motion of the V_O has a high degree of cooperativity below T_3.

IV. DISCUSSION

Figure 5 shows the transition temperatures T_1, T_2, and T_3 plotted versus Y doping in both the fully hydrated and outgassed states. The temperatures T_2 and T_3 are determined from both the real parts $s'(T)$ in Fig. 3 and the respective

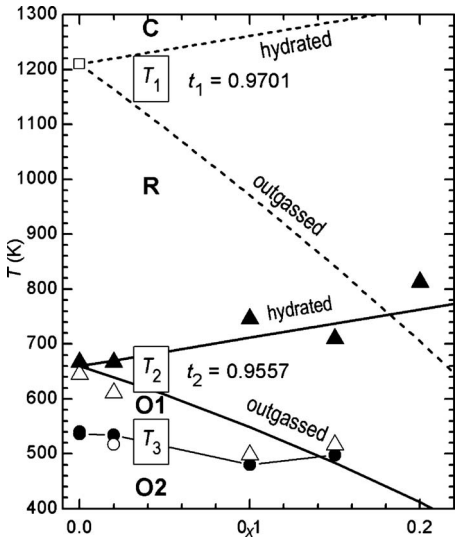

FIG. 5. Temperatures of the three structural transformations of BCY in the hydrated (filled symbols) and outgassed (open symbols) states: R-C square, O1-R triangles, and O2-O1 circles. The thick filled and dashed lines are calculated as explained in the text.

$Q^{-1}(T)$ curves (not reported here) while T_1 is determined from Fig. 1. The O1-R phase transformation is the better characterized in the present measurements and exhibits the largest dependence on doping: an increase in T_2 with doping in the hydrated state and an even larger decrease in the outgassed state. Notice that there is a difference of nearly 30 K between outgassed and hydrated state even at $x=0$, which may be due to the contribution of electronic compensation or to the presence of some defects, e.g., from nonperfect stoichiometry. The transition at T_3 between the two orthorhombic structures is less affected by doping and by O stoichiometry. Differently from that at T_2, it decreases slightly its temperature with doping in the hydrated state, while only at $x=0.02$ it was possible to verify the lowering of the transition temperature after outgassing, because of the masking effect of the transition at T_2.

The R-C transformation has only one point for the undoped case, because our results are only partial and preliminary, due to the experimental difficulties explained in Sec. II. In addition, our anelastic experiments are made in high vacuum, so that above 800 K it is impossible to maintain the sample in the hydrated state, and we can only measure reliably the temperature T_1 of BCY in the outgassed state. Also in the literature there are no data on T_1 of doped BCY.

In what follows we will try to explain the fact that the temperature $T_2(x)$ increases with Y doping x in the hydrated state, and instead decreases with x of an even larger amount in the outgassed state. The uncertainty in the values of T_2 in Fig. 5 is smaller than the symbol size, and the fact that the points at $x=0.10$ and 0.15 do not follow a monotonic trend with doping is likely real and not an experimental vagary. This anomaly can be put in relation with the observation of a jump or extremum in the doping dependence of several structural parameters of $BaCeO_{3-\delta}$ and $SrCeO_{3-\delta}$ at a nominal concentration of V_O $\delta \sim 1/16$,[13] corresponding to $\delta=2x=1/8$ in the fully outgassed state. This phenomenon has been tentatively attributed to ordering of the V_O commensurate with the lattice during the synthesis at high temperature, hence with possible ordering of the cation dopants that would affect the hydration properties also at lower temperature.[13] We will ignore this local inversion of the variation in $T_2(x \simeq 1/8)$, and only consider the positive average derivative of $T_2(x, \delta=0)$ with respect to x and negative derivative of $T_2(x, \delta=x/2)$.

In searching for the relevant factors determining T_2, we note that the O1-R transition involves tilting of the O octahedra, without the atomic off-centering accompanying the ferroelectric transitions or additional Jahn-Teller distortions, since neither Ce^{4+} nor Y^{3+} is Jahn-Teller active. BCY is also inert from the magnetic point of view so that we conclude that the main driving force for the octahedra to tilt is the mismatch between too long B-O bonds (B=Ce/Y) and too short A-O bonds (A=Ba), as usual for ABO_3 perovskites.[19] The tendency of perovskites to undergo tilting transitions is often expressed in terms of the tolerance factor

$$t = \frac{r_A + r_O}{\sqrt{2}(r_B + r_O)}, \tag{2}$$

where the mean ionic radii are the effective ones usually taken from Shannon's tables.[20] A value $t=1$ means that the ideal A-O and B-O bond lengths, taken as the sums of the ideal ionic radii, perfectly match the cubic structure, and therefore that the cubic phase should be stable; $t<1$ means that the B-O bond length is too large with respect to the A-O one, and therefore that the octahedra tend to rotate in order to accommodate the mismatch. The longer and weaker A-O bonds have larger thermal expansion than the shorter and stronger B-O bonds. For this reason, perovskites with $t<1$ already at high temperature further decrease t on cooling, until the mismatch between too long B-O and too short A-O bonds is relived by a tilting structural transformation. Usually, with decreasing t below 1, one finds first tilt patterns producing a more symmetric rhombohedral structure and then the more distorted orthorhombic structures.[19,21] In this respect, $BaCeO_3$ behaves normally, with the cubic phase transforming into rhombohedral $R\bar{3}c$ and further into orthorhombic O1 (*Imma*) and O2 (*Pnma*). The tilt patterns in Glazer's notation[1,22] are, respectively, $a^-a^-a^-$, $a^0b^-b^-$, and $a^+b^-b^-$, and the anomaly in the sequence of transformations is the intermediate loss of a tilt system passing from $a^-a^-a^-$ to $a^0b^-b^-$. Yet, the general trend of C, R, and O structures with decreasing t is obeyed, and the final $a^+b^-b^-$ tilt system is the usual ground state of tilted perovskites,[23] also favored by the slightly covalent component of the A-O bonds.[24,25] It can be concluded that the tolerance factor should be the relevant parameter in promoting the structural transformations in BCY. Another indication in this sense is the fact that $SrCeO_3$, having a still smaller t due the smaller Sr ionic radius, remains in the O2 phase at least up to 1270 K.[26]

It has been noted that, in perovskites with cation chemical disorder in the A sublattice, the temperatures of the structural, and especially magnetic and electronic transitions appear to be sensitive to both the tolerance factor, which measures the coherent strain effect, and the variance of the A

TABLE I. Ionic species of BCY and their molar fractions, radii, and coordination numbers, according to Shannon.

Ion	Molar fraction	Radius (Å)	CN
Ba^{2+}	1	1.61	12
Ce^{4+}	$1-x$	0.87	6
O^{2-}	$3-\delta-y$	1.35	2
Y^{3+}	x	0.90	6
V_O	δ	1.35	
OH^-	y	1.32	2

cation sizes, which measures the incoherent part.[21] In the present case we are dealing only with structural transformations, without the additional critical dependence on the bond angles involved in the electronic and magnetic transitions, and we will just take into account the average effects included in t.

For the limited objective of understanding the effect of doping and hydration on the structural transformations, but not their detailed nature, we keep the analysis as simple as possible, following the idea that the driving force for the nth tilting transition is the decrease in t below some critical value t_n, and therefore that the transition temperatures are proportional to such a driving force,

$$T_n(x) = \Delta T \times [t_n - t(x)]. \tag{3}$$

The dependence of t on x can be estimated by assuming Vegard's law, namely, that the introduction of a molar concentration x of defects, each contributing with a change δv to the ionic volume, causes an isotropic volume change equal to $\Delta V = \delta v x$. In addition we consider a purely ionic picture with each ion having its nominal valence. The ionic species and their molar fractions, coordination numbers, and radii are listed in Table I.

Notice that there is no difference between the use of ionic and crystal radii of the Shannon tables,[20] since they all differ by ± 0.14 Å, depending whether they are anions or cations, and the A-O and B-O ideal distances are unaffected by the choice. The tolerance factor of undoped $BaCeO_3$ resulting from Table I, to be considered as referred to the O2 room-temperature structure, is $t_0 = 0.9428$. Dealing with complete outgassing or hydration, we discard the electronic compensation and assume that the chemical formula of BCY with δV_O and $\frac{y}{2}H_2O$ is $Ba^{2+}Ce^{4+}_{1-x}Y^{3+}_x O^{2-}_{3-\delta-y}OH^-_y$, with the charge compensation requiring

$$2\delta + y = x.$$

Hydrated and outgassed states are therefore defined by $y=x$, $\delta=0$ and $y=0$, $\delta=x/2$, respectively. The proton is assumed to form the hydroxide complex $(OH)^-$, whose radius is also tabulated. The assumption is corroborated by the observation that H fills the hole at the top of the bonding Ce $4f$-O $2p$ valence band, mostly of O $2p$ character, which is introduced by trivalent doping in dry atmosphere.[27] Certainly, the approximation of a spherical $(OH)^-$ ion is inadequate but this is discussed later on.

The tolerance factor of doped BCY can then be written as

$$t = \frac{1}{\sqrt{2}} \frac{\langle d_{AO} \rangle}{\langle d_{BO} \rangle}$$

with

$$\langle d_{AO} \rangle = r_{Ba} + (1 - y/3) r_O + y/3 r_{OH} = d^0_{AO} + \frac{y}{3} \Delta r_O,$$

$$\langle d_{BO} \rangle = (1-x) r_{Ce} + x r_Y + (1 - y/3) r_O + y/3 r_{OH}$$

$$= d^0_{BO} + x \Delta r_B + \frac{y}{3} \Delta r_O,$$

where $\Delta r_B = r_Y - r_{Ce} > 0$, $\Delta r_O = r_{OH} - r_O < 0$ is not very influent because it appears in the same manner in the numerator and denominator of t, and the presence of V_O is not taken into account yet. It is sometimes assumed that the radius of an V_O in a perovskite is the same as that of the O^{2-} ion,[28] and the fact that O deficient perovskites such as $LaCoO_{3-\delta}$ increase their volume with increasing δ is attributed to the enhanced radius of the reduced B cation.[28–30] In the present case, it is evident that a similar assumption would not explain the marked depression of the transition temperatures of the outgassed state with respect to the hydrated and the undoped states. Such a depression would require an increase in t in Eq. (3), which is not supported by any indication. The reduction in T_n must arise from the elimination of the B-O-B and A-O-A bonds, whose rigid networks compete against each other, with expansive and compressive pressures, respectively. The introduction of V_O therefore relaxes the driving force for the tilting structural transformations, reducing it by an amount $R(\delta)$. In the absence of a more detailed and quantitative estimate of the structural relaxation introduced by V_O, we will assume that $R(\delta) = (1 - f\delta)$, resulting in

$$T_n = \Delta T \times (t_n - t)(1 - f\delta), \tag{4}$$

where f is a parameter that quantifies the amount of lattice relaxation associated with V_O; $f = 1/3$ would correspond to a situation in which a tilting driving force exists even with few sparse bonds, and therefore it must be $f \gg 1/3$. The value of f, or more properly the shape of the function $R(\delta)$, and particularly the value of δ at which it vanishes, should be connected with the critical concentration of V_O at which continuum sequences of bonds disappear over some length scale. Yet, there are many factors involved, for example, at $\delta = 0.5$ there might be ordering into the brownmillerite structure,[31,32] and vanishing of $R(\delta)$ at $\delta = 0.5$ would correspond to $f = 2$. We will leave f as a free parameter whose value must be $\gg 1/3$.

From Eq. (4) we may analyze the various factors producing a variation in T_n with doping and hydration. In the hydrated state $R = 1$ and the relevant quantity is, to first order in the changes in the ionic radii,

$$\frac{d(t_n - t)}{dx} \simeq \left[\frac{\Delta r_B}{d^0_{BO}} + \frac{\Delta r_O}{3} \left(\frac{1}{d^0_{BO}} - \frac{1}{d^0_{AO}} \right) \right] t_0, \tag{5}$$

where the first positive term, representing the average increase in the B radius on doping, is dominant. The second

term is reduced by a geometrical factor $\simeq\frac{1}{3}(1-1/\sqrt{2})\simeq 0.1$, and therefore the most questionable assumption of adopting the tabulated radius for the hydroxide ion is not important. From Eqs. (4) and (5) we obtain the proportionality factor between tilting driving force and structural transition temperature, as

$$\Delta T = \frac{\left.\frac{dT_n}{dx}\right|_{\mathrm{hydr}}}{\left.\frac{d(t_n - t)}{dx}\right|_{\mathrm{hydr}}}.$$

Setting $\left.\frac{dT_2}{dx}\right|_{\mathrm{hydr}}=520$ K we obtain $\Delta T=44\ 300$ K and extract the critical tolerance factor t_2 for the O1-R transition at $T_2=660$ K in the undoped case from Eq. (4) as $t_2=0.9577$. Finally, the parameter f is deduced from the initial slope of $\left.\frac{dT_2}{dx}\right|_{\mathrm{outg}}\simeq -1100$ K as

$$f = \frac{2}{(t_2 - t_0)}\left[\frac{\Delta r_{\mathrm{B}}}{d^0_{\mathrm{BO}}}t_0 - \frac{\left.\frac{dT_2}{dx}\right|_{\mathrm{outg}}}{\Delta T}\right] = 5.0.$$

The resulting $T_2(x)$ curves in the hydrated and outgassed states are plotted as thick solid lines in Fig. 5. There is some arbitrariness in the choice of the initial slopes of the curves, due to the above mentioned anomaly between $x=0.1$ and 0.15, but the main features can be reproduced with reasonable parameters. This simple reasoning might be applied also to the other two transitions at T_1 and T_3, with different values for the critical tolerance factors $t_1>t_2>t_3$ and possibly also for the proportionality factor ΔT, because the different structures relax the mismatch between *A*-O and *B*-O sublattices at varying degrees. The dashed lines in Fig. 5 are obtained letting ΔT and f unchanged and setting $t_1=0.9701$ in order to reproduce $T_1(0)=1210$ K. It is reassuring to find that t_1 is exactly at the lower limit of the range $0.97<t<1$ where cubic perovskites are found.[33] There are no data for T_1 in the hydrated state while for the outgassed state there are only preliminary anelastic spectra suggesting that at $x=0.15$ it is $T_1\gtrsim 950$ K, about 100 K higher than the dashed line. We refrain from speculating whether this would be due to a larger value of ΔT for that transition or to other reasons that are not included in the present minimal model.

Additional factors are likely present in the O1-O2 transition at T_3, whose temperature even decreases slightly on doping, maintaining the anomaly between $x=0.10$ and 0.15. Yet, the effect of V_O is again to depress the transition temperature, although this is verifiable only at $x=0.02$, due to the overlapping with the O1-R transformation. Among the phenomena interfering with the O1-O2 transition is the ordering of the V_O. In fact, while the V_O are disordered in their three equivalent O sublattices in the rhombohedral structure and also in the orthorhombic O1, they are confined to only two sublattices, avoiding the third crystallographically inequivalent sublattice, in the O2 structure.[1,12] It is not clear whether V_O ordering is concomitant with the transition or it occurs at a slower rate after the transition is completed. We have already noted[15] that a possible sign of cooperative ordering of V_O is the anelastic relaxation process labeled as R6, whose intensity seems to diverge on approaching T_2 from below, as expected from critical ordering of the elastic quadrupoles associated with the V_O.[34–36] A similar divergence of the relaxation strength Δ is shown in Fig. 4 for peak RV. In the framework of the Bragg-Williams approximation,[37] the critical temperature for the onset of ordering of V_O is expected to scale as[35,36] $\delta(1-\delta)$ and therefore to increase with doping, possibly driving the O2-O1 transformation to higher temperature and explaining the apparently reduced decrease in $T_3(x,\delta=x/2)$ with respect to $T_3(x,\delta=0)$, compared to T_2.

The fact that the decrease in T_3 in the hydrated state is smaller then for T_2, instead, must involve completely different mechanisms. A possibility is that on cooling the proton localizes itself more and more within the plane perpendicular to the *B*-O-*B* bond,[1,12,38] effectively resulting in an increased flattening of the hydroxide ion and hence in a reduction in its effective radius along the *B*-O-*B* bond direction. Such an effect, namely, an additional reduction in the *B*-OH-*B* but not of the *A*-OH-*A* bond lengths on cooling, would reduce the mismatch between the two bond networks and result in a stabilization of the higher temperature phase, hence a decrease in T_3.

Finally, let us compare these dependencies of the transition temperatures on Y doping with those measured by XRD and dilatometry with Yb doping.[9] Those data have been considered insufficient,[2] due to the smallness of the anomalies in the linear expansion, which also exhibit an additional dip not associated with any phase transformation, and the limited number of diffraction peaks that were analyzed. Yet, Yamaguchi and Yamada[9] plotted T_1, T_2, and T_3 versus Yb doping measured both under wet and dry conditions, as in our Fig. 5. Similarly to the present results, the T_n in dry atmosphere are lower than those under in wet atmosphere, especially for $x\geq 0.1$ but to a lesser extent than in Fig. 5. The main difference between the two sets of experiments is that $T_2(x)$ with Yb has a much weaker rise with doping than with Y and only for $x\geq 0.1$ while $T_1(x)$ even decreases with doping. This difference can also be explained within the above model since the radius of Yb^{3+} is slightly smaller than that of Ce^{4+}, instead of larger as for Y^{3+}, so that with Yb it is $\Delta r_{\mathrm{B}}=-0.003$ Å instead of +0.03 Å.

V. CONCLUSIONS

The temperatures T_n of the structural transformations in BCY have been systematically deduced from the anelastic spectra as a function of Y doping x and hydration level y, or O deficiency δ. The most complete data are for the intermediate transition between orthorhombic *Imma* and rhombohedral at T_2; the data of the transition at the lowest temperature T_3 to the orthorhombic *Pnma* phase are incomplete in the outgassed state, due to overlapping with the transition at T_2, whose effects prevail in the anelastic spectra. Of the transition to the cubic phase we could measure only the temperature $T_1=1210$ K in the undoped state.

The main result is that $T_2(x)$ increases roughly as $(500\ \mathrm{K})\times x$ in the fully hydrated state and decreases twice as much in the fully outgassed state. An anomaly with respect to the monotonic trend between $x=0.10$ and 0.15 is

associated with similar anomalies already observed in various structural parameters at the same doping level while the average trend is explained with a simple model. As usual, it is assumed that the main driving force for the structural transformations, which consist of rotations of the BO_6 octahedra (B=Ce, Y), is the mismatch between the more rigid and compressed network of B-O-B bonds and the network of Ba-O-Ba bonds under expansion. The transition temperatures T_n are assumed to be proportional to $(t_n - t)(1 - f\delta)$, where t is the tolerance factor measuring the ratio between the ideal Ba-O and B-O bond lengths, t_n a critical value of t below which the nth tilting transition occurs, and f a parameter determined by how much the mismatch stress between different types of bonds is relieved by the presence of O vacancies. In this manner it is possible to explain the experimental $T_2(x, \delta)$ data with reasonable parameters, and also to reproduce $T_1(x=0)$ with $t_1=0.97$, which is just the lower limit of the known range $0.97 < t < 1$ for cubic perovskites.

The transition temperature T_3, instead, decreases with doping and has a reduced difference between hydrated and outgassed states. These differences with respect to $T_2(x, \delta)$ are tentatively explained in terms of a reduction in the mismatch between the bond lengths, due to a flattening of the effective shape of the hydroxide ion perpendicularly to the B-O-B bond during cooling, and to the ordering of the O vacancies in the *Pnma* phase.

ACKNOWLEDGMENTS

We wish to thank F. Corvasce, M. Latino, and A. Morbidini for their technical assistance, and Ing. E. Verona and co-workers of CNR-IDASC for the Pt depositions. This research is supported by the FISR Project of Italian MIUR: "Celle a combustibile ad elettroliti polimerici e ceramici: dimostrazione di sistemi e sviluppo di nuovi materiali."

[1] K. S. Knight, Solid State Ionics **145**, 275 (2001).
[2] T. Ohzeki, S. Hasegawa, M. Shimizu, and T. Hashimoto, Solid State Ionics **180**, 1034 (2009).
[3] C. N. W. Darlington, Phys. Status Solidi A **155**, 31 (1996).
[4] K. D. Kreuer, Solid State Ionics **97**, 1 (1997).
[5] P. Berastegui, S. Hull, F. J. Garcia-Garcia, and S.-G. Eriksson, J. Solid State Chem. **164**, 119 (2002).
[6] T. Nagai, W. Ito, and T. Sakon, Solid State Ionics **177**, 3433 (2007).
[7] G. Chiodelli, L. Malavasi, C. Tealdi, S. Barison, M. Battagliarin, L. Doubova, M. Fabrizio, C. Mortalo, and R. Gerbasi, J. Alloys Compd. **470**, 477 (2009).
[8] Yu. M. Baikov, V. M. Egorov, N. F. Kartenko, B. A.-T. Melekh, Yu. P. Stepanov, and Yu. N. Filin, Tech. Phys. Lett. **24**, 782 (1998).
[9] S. Yamaguchi and N. Yamada, Solid State Ionics **162-163**, 23 (2003).
[10] T. Scherban, R. Villeneuve, L. Abello, and G. Lucazeau, Solid State Ionics **61**, 93 (1993).
[11] K. S. Knight, Solid State Commun. **112**, 73 (1999).
[12] K. Takeuchi, C.-K. Loong, J. W. Richardson, Jr., J. Guan, S. E. Dorris, and U. Balachandran, Solid State Ionics **138**, 63 (2000).
[13] A. Kruth, G. C. Mather, J. R. Jurado, and J. T. S. Irvine, Solid State Ionics **176**, 703 (2005).
[14] F. Giannici, A. Longo, F. Deganello, A. Balerna, A. S. Arico, and A. Martorana, Solid State Ionics **178**, 587 (2007).
[15] F. Cordero, F. Trequattrini, F. Deganello, V. La Parola, E. Roncari, and A. Sanson, Appl. Phys. Lett. **94**, 181905 (2009).
[16] F. Cordero, F. Craciun, F. Deganello, V. La Parola, E. Roncari, and A. Sanson, Phys. Rev. B **78**, 054108 (2008).
[17] F. Deganello, G. Marcì, and G. Deganello, J. Eur. Ceram. Soc. **29**, 439 (2009).
[18] A. S. Nowick and B. S. Berry, *Anelastic Relaxation in Crystalline Solids* (Academic Press, New York, 1972).
[19] J. B. Goodenough, Rep. Prog. Phys. **67**, 1915 (2004).
[20] R. D. Shannon and C. T. Prewitt, Acta Crystallogr., Sect. B: Struct. Crystallogr. Cryst. Chem. **25**, 925 (1969).
[21] J. P. Attfield, Int. J. Inorg. Mater. **3**, 1147 (2001).
[22] A. M. Glazer, Acta Crystallogr., Sect. B: Struct. Crystallogr. Cryst. Chem. **28**, 3384 (1972).
[23] P. Goudochnikov and A. J. Bell, J. Phys.: Condens. Matter **19**, 176201 (2007).
[24] J. B. Goodenough and J. A. Kafalas, J. Solid State Chem. **6**, 493 (1973).
[25] P. M. Woodward, Acta Crystallogr., Sect. B: Struct. Sci. **53**, 32 (1997).
[26] K. S. Knight, W. G. Marshall, N. Bonanos, and D. J. Francis, J. Alloys Compd. **394**, 131 (2005).
[27] T. Higuchi, T. Tsukamoto, H. Matsumoto, T. Shimura, K. Yashiro, T. Kawada, J. Mizusaki, S. Shin, and T. Hattori, Solid State Ionics **176**, 2967 (2005).
[28] A. Yu. Zuev, A. I. Vylkov, A. N. Petrov, and D. S. Tsvetkov, Solid State Ionics **179**, 1876 (2008).
[29] K. Hilpert, R. W. Steinbrech, F. Boroom, E. Wessel, F. Meschke, A. Zuev, O. Teller, H. Nickel, and L. Singheiser, J. Eur. Ceram. Soc. **23**, 3009 (2003).
[30] V. V. Kharton, A. V. Kovalevsky, E. V. Tsipis,A. P. Viskup, E. N. Naumovich, J. R. Jurado, and J. R. Frade, J. Solid State Electrochem. **7**, 30 (2002).
[31] A. F. Sammells, R. L. Cook, J. H. White, J. J. Osborne, and R. C. MacDuff, Solid State Ionics **52**, 111 (1992).
[32] G. B. Zhang and D. M. Smyth, Solid State Ionics **82**, 161 (1995).
[33] M. W. Lufaso, P. W. Barnes, and P. M. Woodward, Acta Crystallogr., Sect. B: Struct. Sci. **62**, 397 (2006).
[34] F. Cordero, M. Ferretti, M. R. Cimberle, and R. Masini, Phys. Rev. B **67**, 144519 (2003).
[35] F. Brenscheidt, D. Seidel, and H. Wipf, J. Alloys Compd. **211-212**, 264 (1994).
[36] F. Cordero, *Anelastic Spectroscopy Studies of High-T_c: Superconductors: Dynamics of Hole Stripes, Oxygen Atoms and Octahedra* (Lambert Academic, Saarbrücken, Germany, 2010).
[37] T. Muto and Y. Takagi, in *Solid State Physics*, edited by F. Seitz and D. Turnbull (Academic Press, New York, 1955), p. 193.
[38] A. K. Azad and J. T. S. Irvine, Chem. Mater. **21**, 215 (2009).